

---

# SCIURus: Shared Circuits for Interpretable Uncertainty Representations in Language Models

---

Anonymous Author(s)

Affiliation

Address

email

## Abstract

1 We investigate the mechanistic sources of uncertainty in large language models  
2 (LLMs), an area with important implications for their reliability and trustworthi-  
3 ness. To do so, we conduct a series of experiments designed to identify whether the  
4 factuality of generated responses and a model’s uncertainty originate in separate or  
5 shared circuits [5] in the model architecture. We approach this question by adapt-  
6 ing the well-established mechanistic interpretability techniques of path patching  
7 and zero-ablation that allows identifying the effect of different circuits on LLM  
8 generations. Our extensive experiments on eight different models and five datasets,  
9 representing tasks predominantly requiring factual recall, clearly demonstrate that  
10 uncertainty is produced in the same parts of a model that are responsible for the  
11 factuality of generated responses. We release code for our implementation.

## 12 1 Introduction

13 Uncertainty quantification (UQ) in large language models (LLMs) for knowledge-intensive tasks  
14 [16] remains a critical yet understudied area. Despite achieving human-level performance on various  
15 benchmarks, LLMs often struggle with reliable uncertainty estimation, leading to issues such as  
16 overconfidence and hallucination [19]. This limitation has strong implications for their trustworthiness  
17 and safety in high-stakes applications. While recent research has explored verbalized uncertainty  
18 in LLMs [1, 10, 11], significant gaps remain in our understanding and ability to improve UQ. In  
19 particular, existing UQ techniques typically provide little insight into the factors responsible for an  
20 uncertainty estimate, limiting their usefulness both as tools for trustworthiness. We propose leveraging  
21 mechanistic interpretability, an approach focused on characterizing models’ internal mechanisms of  
22 reasoning, to advance our comprehension and enhancement of uncertainty quantification in LLMs.

23 Following Kadavath et al. [10], to better understand how LMs generate uncertainty estimates, we used  
24 parametric  $\mathbb{P}(\text{IK})$  (“probability that I know”) probes—one-layer binary classifiers that are trained to  
25 predict the probability that a given LM knows the answer to a given question. As in [10], we trained  
26  $\mathbb{P}(\text{IK})$  probes on several datasets and with several models. We then used these probes’ predicted  
27 confidences as target metrics for path patching and zero-ablation, two mechanistic interpretability  
28 techniques which identify the components of a model relevant for a task by testing the effect of an  
29 interventions made on activations in the model during evaluation. We compared the mechanistic  
30 signatures of changes in the model’s accuracy and the probe’s output to evaluate whether the same  
31 circuits were responsible for the answer and the predicted confidence.

32 In our empirical evaluation, in which we performed zero-ablation for a large range of model–dataset  
33 combinations and path patching for one combination, we found that model accuracy and probe  
34 behavior largely responded to the same interventions, indicating that circuits responsible for the  
35 factuality of responses and for uncertainty quantification are located in the same parts of the model.

36 For a group of knowledge-intensive question answering [16] tasks, model accuracy and probe  
37 confidence are (highly) positively related to one another. We conclude that, at least on recall tasks, a

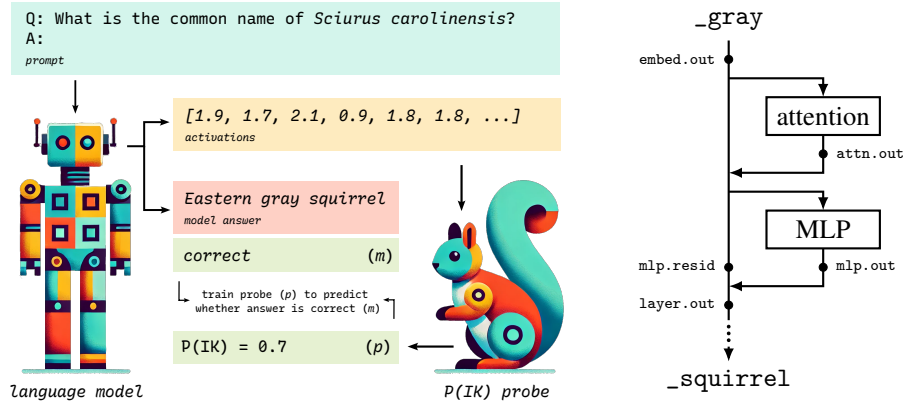


Figure 1: **Left:**  $\mathbb{P}(IK)$  probing. The LLM takes a question as input and returns an answer and last-layer activations. Answers are checked for correctness. The probe learns to predict whether the model’s answer is correct, based on the last-layer activations. Our analysis uses the probe as a proxy for an LLM’s  $\mathbb{P}(IK)$ . We conduct path patching and zero ablation studies on the probe and the corresponding LLM. **Right:** Locations used in interventions. Path-patching restorations are at `mlp.resid`, `mlp.out`, `layer.out`, and `embed.out`. Zero-ablations are at `attn.out` and `mlp.out`.

38 language model’s representation of confidence may derive mainly from introspection on its question-  
 39 answering process, rather than from separate reasoning specific to the UQ task.

40 To summarize, the key contributions of this paper are as follows:

- 41 1. We use mechanistic interpretability and uncertainty quantification tools to investigate the mecha-  
 42 nistic sources of uncertainty in large language models. To do so, we use a logistic  $\mathbb{P}(IK)$  probe  
 43 with path patching and zero-ablation to perform a hypothesis test to examine whether LLM  
 44 uncertainty and the factuality of answers generated by an LLM reside in shared or separate  
 45 circuits within the model.
- 46 2. We perform an extensive empirical analysis on eight different models and five recall-intensive  
 47 datasets, and find evidence that uncertainty quantification and the factuality of answers generated  
 48 by an LLM are handled by the same parts of the model.

## 49 2 Background

50 **Path Patching.** Path patching is a causal intervention method that aims to trace and identify  
 51 important components in neural models for a given task [14, 18], which is a generalization of causal  
 52 mediation analysis [17]. In this work, we use path patching [14] to examine the importance and role  
 53 of individual circuits and components in LLMs. Specifically, given a specific input  $q$ , path patching  
 54 involves three runs: (1) a clean run, in which the original input  $q$  is given to the model, which is  
 55 used to obtain the hidden states of each layer; (2) a corrupted run, in which the input embeddings  
 56 of certain tokens are corrupted by adding noise or (in this paper) replaced with zeros; and (3) a  
 57 corrupted-with-restoration run, in which the computation is similar to the corrupted run except that  
 58 the hidden states at specific locations  $\ell$  in the model are restored using the hidden states obtained  
 59 from the clean run. By comparing the differences between the output (predicted probabilities) of the  
 60 clean, corrupted, and restored runs, path patching allows the identification of important components  
 61 in LLMs. That is, if the restored run achieves a similar effect as the clean run, it is likely that the  
 62 corresponding restored component plays an important role in the model’s processing.

63 **Zero-Ablation.** Zero-ablation is a mechanistic intervention technique that takes advantage of a  
 64 transformer’s residual structure by treating attention or MLP layers as separable modules which read  
 65 from and write to the residual stream [6, 15]. A component  $\ell$  (in this paper, an attention or MLP  
 66 layer) is “ablated” by replacing its output with zero. The drop in model performance on a given task  
 67 after an intervention removing a component  $\ell$  provides a measure of the importance of  $\ell$  for the task.

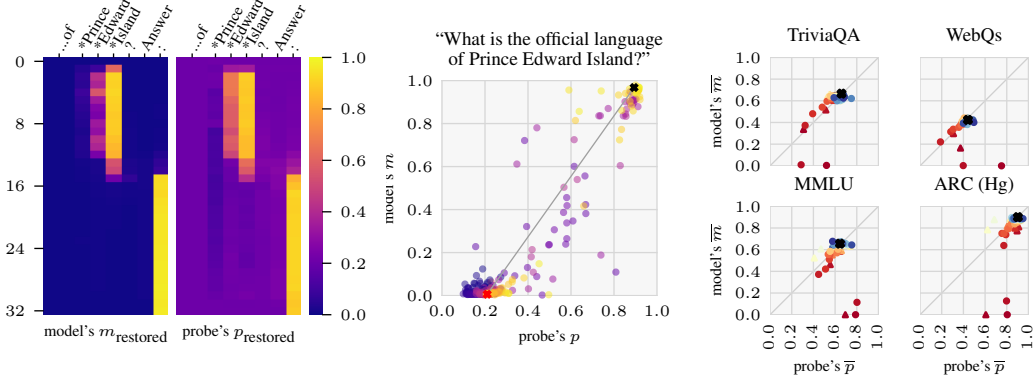


Figure 2: **Left:** Results of path patching for Llama 3 8B Instruct on a question in CounterFact. Only layer .out locations are shown (plus embed.out in the first row). The input embeddings for the starred tokens are replaced with zeros in the corrupted and restored runs. **Center:** Predicting  $m$  given  $p$ . The black and red X (top-right and bottom-left) show the clean and corrupted runs; all others show restored runs. Yellow points are later in the sequence. The grey line shows the predictor  $\hat{m}$ . **Right:** Results of zero ablation for Llama 3 8B Instruct on four different datasets. Circle, triangle, and X markers represent MLP ablations, attention ablations, and clean runs respectively. Warmer colors represent earlier layers.

### 68 3 Uncertainty Introspection: Investigating the Shared Circuits Hypothesis

69 The aim of this paper is to make progress toward characterizing the mechanistic structures used for  
 70 UQ in language models. To this end, we propose a theoretical hypothesis (“shared circuits”) about  
 71 the locations of these structures, along with operationalizations which we test experimentally.

**Shared Circuits Hypothesis.** Uncertainty quantification in question-answering (QA) systems may be carried out in a variety of ways. We hypothesize that language models are capable of expressing uncertainty using **shared circuits** that both solve the underlying question-answering task and output uncertainty information. This contrasts with the possibility that uncertainty quantification emerges in **separate circuits**, either to post-process messy uncertainty signals from question-answering circuits or to do uncertainty calculations of their own.

72  
 73 We study eight Llama[12, 13] and Gemma [7] models and five datasets, described in Appendix ??.

#### 74 3.1 Experiment Design: Path Patching

75 On a given question  $q_i$  in a dataset  $\mathcal{Q}$ , for each path patching run (clean, corrupted, and restored)  
 76 we compute the model’s sample probability  $m(q_i)$  for the correct first token of the answer, and  
 77 the probe’s confidence  $p(q_i)$ . (We omit the question for the rest of this section for legibility; we  
 78 consider questions individually.) Locations  $\ell$  where  $m_{\text{restored}(\ell)} \approx m_{\text{clean}}$  correspond to parts of the  
 79 model which are important for solving the QA task; likewise, locations  $\ell$  where  $p_{\text{restored}(\ell)} \approx p_{\text{clean}}$   
 80 correspond to parts of the model which are important for the UQ task.<sup>12</sup> In the context of path  
 81 patching, we operationalize the shared circuits hypothesis in the claim that  $m_{\text{restored}}$  can be predicted  
 82 from  $p_{\text{restored}}$  by interpolating between the clean and corrupted values: for example, if the model’s  
 83 correct-token probability on a restored run is halfway between the values from the clean and corrupted  
 84 runs, then the probe’s confidence should also be halfway between the clean and corrupted runs.

85 Specifically, for each question  $q_i \in \mathcal{Q}$ , we claim that the linear predictor  $\hat{m}_{\text{restored}}$  defined by

$$\frac{\hat{m}_{\text{restored}(\ell)} - m_{\text{corrupted}}}{m_{\text{clean}} - m_{\text{corrupted}}} = \frac{p_{\text{restored}(\ell)} - p_{\text{corrupted}}}{p_{\text{clean}} - p_{\text{corrupted}}}$$

<sup>1</sup>Although note that the converse is not necessarily true; see Appendix D for details.

<sup>2</sup>Here,  $\mathbb{P}(\text{corr})_{\text{restored}(\ell)}$  and  $\mathbb{P}(\text{IK})_{\text{restored}(\ell)}$  represent the correct token probability and  $p$  probe output for a run with the hidden state restored at location  $\ell$  in the model; notation is likewise for clean and corrupted runs.

86 explains most of the variance in  $m_{\text{restored}}$  (i.e., has a high coefficient of determination  $R^2$ ). As a  
87 (somewhat weak) formalization of this, we attempt to reject the null hypothesis

$$H_0 : R^2 \text{ is no greater than expected under random permutations of the set of locations } \ell. \quad (1)$$

### 88 3.2 Experiment Design: Zero-Ablation

89 We also test the shared circuits hypothesis via zero-ablation on layers. Here, because we are interested  
90 in multi-token answers, we define  $m(q_i)$  as the probability of a correct answer sampled by the model  
91 when prompted on the question  $q_i \in \mathcal{Q}$ , and  $p(q_i)$  as the probe output on that question. Taking means  
92 over  $\mathcal{Q}$ , we can compare changes in the model accuracy  $\bar{m}$  and the average probe output  $\bar{p}$ . Under  
93 the shared circuits hypothesis, the change in the probe output from ablation  $|\bar{p}_{\text{ablated}(\ell)} - p_{\text{clean}}|$  is  
94 large when the change in model accuracy  $|\bar{m}_{\text{ablated}(\ell)} - m_{\text{clean}}|$  is large. Concretely, we claim that the  
95 predictor  $\hat{m}$  defined by

$$m_{\text{clean}} - \hat{m}_{\text{ablated}(\ell)} = |\bar{p}_{\text{ablated}(\ell)} - p_{\text{clean}}|$$

96 explains most of the variance in  $\bar{m}_{\text{ablated}}$  (has a high  $R^2$ ), and attempt to reject the null hypothesis

$$H_0 : R^2 \text{ is no greater than expected under random permutations of the set of layers } \ell. \quad (2)$$

### 97 3.3 Testing the Hypothesis

98 **Path Patching.** We performed path patching with Llama 3 8B Instruct [13] on a random sample of  
99 16 questions from the CounterFact dataset [14], considering only questions which the model could  
100 answer ( $m_{\text{clean}} > 0.5$ ). We used the probe and few-shot prompt for TriviaQA. Across this sample,  
101 the predictors  $\hat{m}_{\text{restored}}$  generally estimated  $m_{\text{restored}}$  well, with  $R^2 > 0.6$  in all but three cases.<sup>3</sup> For  
102 each question  $q_i$ , we tested the null hypothesis (1) by sampling 10,000 permutations.<sup>4</sup> In all cases,  
103 we reject  $H_0$  with  $p < 0.0001$ .

104 **Zero-Ablation.** We performed zero ablation with eight models across five question-answering  
105 datasets (see Appendix B). Across this sample, the predictors  $\hat{m}_{\text{ablated}}$  generally estimated  $\bar{m}_{\text{ablated}}$   
106 better than chance, with a median of  $R^2 = 0.33$ . For each model–dataset combination, we tested the  
107 null hypothesis (2) by sampling 10,000 permutations. We reject the null hypothesis with  $p < 0.05$  in  
108 36 out of 38 cases, and  $p < 0.0001$  in 31 out of 38 cases.

109 In many cases, the model’s uncertainty representation plays particularly nicely with zero-ablation,  
110 remaining calibrated on average even after an intervention: using the same statistical framework  
111 as above, the very simple predictor  $\hat{m}_{\text{ablated}} = \bar{p}_{\text{ablated}}$  does better than expected under random  
112 permutations in 27 out of 38 cases (at  $p < 0.05$ ).<sup>5</sup> While other explanations may be possible, one  
113 interpretation of these results is that a given component makes a nonzero contribution to the model’s  
114 uncertainty representation if and only if it can also contribute information about the answer.

## 115 4 Discussion and Conclusion

116 The results of our path patching and zero-ablation analyses broadly support the shared circuits  
117 hypothesis, implying that across the setups we considered the sets of model components used for  
118 question-answering and uncertainty quantification were largely, albeit not entirely, the same. This  
119 suggests that  $\mathbb{P}(\text{IK})$  probing may be a viable way of eliciting introspective, interpretable uncertainty  
120 estimates. Based on these findings, further research could analyze the mechanisms responsible  
121 for  $\mathbb{P}(\text{IK})$  estimates in greater detail or apply  $\mathbb{P}(\text{IK})$  probing as an interpretability tool to study  
122 phenomena such as hallucination in LLMs and meaningfully contribute to technical AI governance.

<sup>3</sup>Based on manual inspection (see graphs in the Supplementary Materials), we conclude that  $R^2 < 1$  both due to small discrepancies between UQ and QA circuitry and due to nonlinearity in the UQ/QA relationship.

<sup>4</sup>Specifically, we shuffle the values of  $m_{\text{restored}(\ell)}$  independently for the `mlp.out`, `mlp.resid`, and `layer.out/embed.out` locations, to exclude the explanation that the predictor works well because the `mlp.out` and `mlp.resid` states each carry less information than `layer.out`. We do likewise for zero-ablation.

<sup>5</sup>If  $R^2$  is the fraction of the variance in  $\bar{m}_{\text{ablated}}$  explained by  $\hat{m}_{\text{ablated}} = \bar{p}_{\text{ablated}}$ , we reject the null hypothesis  $R^2$  is no greater than expected under random permutations of the set of layers  $\ell$  at  $p < 0.05$  in 27/38 cases.

## References

- 123
- 124 [1] Neil Band, Xuechen Li, Tengyu Ma, and Tatsunori Hashimoto. Linguistic calibration of  
125 long-form generations. In *Forty-first International Conference on Machine Learning*, 2024.
- 126 [2] Jonathan Berant, Andrew Chou, Roy Frostig, and Percy Liang. Semantic parsing on Freebase  
127 from question-answer pairs. In *Proceedings of the 2013 Conference on Empirical Methods in  
128 Natural Language Processing*, pages 1533–1544, Seattle, Washington, USA, October 2013.  
129 Association for Computational Linguistics.
- 130 [3] Lawrence Chan, Adrià Garriga-Alonso, Nicholas Goldowsky-Dill, Ryan Greenblatt, Jenny,  
131 Ansh Radhakrishnan, Buck Shlegeris, and Nate Thomas. Causal scrubbing: A method for  
132 rigorously testing interpretability hypotheses, December 2022.
- 133 [4] Peter Clark, Isaac Cowhey, Oren Etzioni, Tushar Khot, Ashish Sabharwal, Carissa Schoenick,  
134 and Oyvind Tafjord. Think you have solved question answering? try arc, the ai2 reasoning  
135 challenge. *arXiv:1803.05457v1*, 2018.
- 136 [5] Nelson Elhage, Neel Nanda, Catherine Olsson, Tom Henighan, Nicholas Joseph, Ben Mann,  
137 Amanda Askell, Yuntao Bai, Anna Chen, Tom Conerly, Nova DasSarma, Dawn Drain, Deep  
138 Ganguli, Zac Hatfield-Dodds, Danny Hernandez, Andy Jones, Jackson Kernion, Liane Lovitt,  
139 Kamal Ndousse, Dario Amodei, Tom Brown, Jack Clark, Jared Kaplan, Sam McCandlish, and  
140 Chris Olah. A mathematical framework for transformer circuits. *Transformer Circuits Thread*,  
141 2021. <https://transformer-circuits.pub/2021/framework/index.html>.
- 142 [6] Nelson Elhage, Neel Nanda, Catherine Olsson, Tom Henighan, Nicholas Joseph, Ben Mann,  
143 Amanda Askell, Yuntao Bai, Anna Chen, Tom Conerly, Nova DasSarma, Dawn Drain, Deep  
144 Ganguli, Zac Hatfield-Dodds, Danny Hernandez, Andy Jones, Jackson Kernion, Liane Lovitt,  
145 Kamal Ndousse, Dario Amodei, Tom Brown, Jack Clark, Jared Kaplan, Sam McCandlish, and  
146 Chris Olah. A mathematical framework for transformer circuits, 2021.
- 147 [7] Gemma Team, Google AI. Gemma 2: Improving open language models at a practical size,  
148 2024.
- 149 [8] Dan Hendrycks, Collin Burns, Steven Basart, Andy Zou, Mantas Mazeika, Dawn Song, and  
150 Jacob Steinhardt. Measuring massive multitask language understanding. *Proceedings of the  
151 International Conference on Learning Representations (ICLR)*, 2021.
- 152 [9] Mandar Joshi, Eunsol Choi, Daniel Weld, and Luke Zettlemoyer. TriviaQA: A large scale  
153 distantly supervised challenge dataset for reading comprehension. In *Proceedings of the 55th  
154 Annual Meeting of the Association for Computational Linguistics (Volume 1: Long Papers)*,  
155 page 1601–1611, Vancouver, Canada, 2017. Association for Computational Linguistics.
- 156 [10] Saurav Kadavath, Tom Conerly, Amanda Askell, Tom Henighan, Dawn Drain, Ethan Perez,  
157 Nicholas Schiefer, Zac Hatfield-Dodds, Nova DasSarma, Eli Tran-Johnson, Scott Johnston,  
158 Sheer El-Showk, Andy Jones, Nelson Elhage, Tristan Hume, Anna Chen, Yuntao Bai, Sam  
159 Bowman, Stanislav Fort, Deep Ganguli, Danny Hernandez, Josh Jacobson, Jackson Kernion,  
160 Shauna Kravec, Liane Lovitt, Kamal Ndousse, Catherine Olsson, Sam Ringer, Dario Amodei,  
161 Tom Brown, Jack Clark, Nicholas Joseph, Ben Mann, Sam McCandlish, Chris Olah, and Jared  
162 Kaplan. Language models (mostly) know what they know, 2022.
- 163 [11] Lorenz Kuhn, Yarín Gal, and Sebastian Farquhar. Semantic uncertainty: Linguistic invariances  
164 for uncertainty estimation in natural language generation. In *Proceedings of the Eleventh  
165 International Conference on Learning Representations*, September 2022.
- 166 [12] Llama 2 Team, Meta AI. Llama 2: Open foundation and fine-tuned chat models, 2023.
- 167 [13] Llama 3 Team, Meta AI. The llama 3 herd of models, 2024.
- 168 [14] Kevin Meng, David Bau, Alex J Andonian, and Yonatan Belinkov. Locating and editing factual  
169 associations in GPT. In Alice H. Oh, Alekh Agarwal, Danielle Belgrave, and Kyunghyun Cho,  
170 editors, *Advances in Neural Information Processing Systems*, 2022.
- 171 [15] Nostalgebraist. Interpreting GPT: The logit lens, August 2020.

- 172 [16] Fabio Petroni, Aleksandra Piktus, Angela Fan, Patrick S. H. Lewis, Majid Yazdani, Nicola De  
173 Cao, James Thorne, Yacine Jernite, Vassilis Plachouras, Tim Rocktäschel, and Sebastian Riedel.  
174 KILT: a benchmark for knowledge intensive language tasks. *CoRR*, abs/2009.02252, 2020.
- 175 [17] Jesse Vig, Sebastian Gehrmann, Yonatan Belinkov, Sharon Qian, Daniel Nevo, Yaron Singer,  
176 and Stuart Shieber. Investigating gender bias in language models using causal mediation  
177 analysis. In H. Larochelle, M. Ranzato, R. Hadsell, M.F. Balcan, and H. Lin, editors, *Advances*  
178 *in Neural Information Processing Systems*, volume 33, pages 12388–12401. Curran Associates,  
179 Inc., 2020.
- 180 [18] Kevin Ro Wang, Alexandre Variengien, Arthur Conmy, Buck Shlegeris, and Jacob Steinhardt.  
181 Interpretability in the wild: a circuit for indirect object identification in GPT-2 small. In *The*  
182 *Eleventh International Conference on Learning Representations*, 2023.
- 183 [19] Muru Zhang, Ofir Press, William Merrill, Alisa Liu, and Noah A. Smith. How language model  
184 hallucinations can snowball. In *Forty-first International Conference on Machine Learning*,  
185 2024.

# 186 Appendix

## 187 Appendix A Reproducibility

Code to reproduce our results can be found at

[https://anonymous.4open.science/r/sciurus\\_anonymized-E434/](https://anonymous.4open.science/r/sciurus_anonymized-E434/)

188

## 189 Appendix B Models and Datasets

We studied the following eight models and five datasets:

Table 1: Models studied

| Model               | Parameters | Layers | Dataset         |
|---------------------|------------|--------|-----------------|
| Llama 2 7B          | 7B         | 32     | TriviaQA[9]     |
| Llama 2 7B Chat     | 7B         | 32     | WebQuestions[2] |
| Llama 2 13B         | 13B        | 40     | MMLU[8]         |
| Llama 2 13B Chat    | 13B        | 40     | ARC[4]          |
| Llama 3 8B          | 8B         | 32     | CounterFact[14] |
| Llama 3 8B Instruct | 8B         | 32     |                 |
| Gemma 2 2B Instruct | 2B         | 26     |                 |
| Gemma 2 9B Instruct | 9B         | 42     |                 |

190

191 All the datasets studied, with the partial exception of MMLU, are “recall-intensive” in that they  
192 largely depend on recalling factual information learned during training. Based on some preliminary  
193 zero-ablation experiments, we believe that models may exhibit separate circuits on some non-recall  
194 tasks such as simple synthetic math questions.

195 ARC includes both the ARC-Easy and ARC-Challenge splits. ARC questions are drawn from  
196 standardized tests; the datasets listed as ARC (Hg) and ARC (Other) correspond, respectively, to the  
197 “Mercury” test and to a combination of the other 20 tests.

198 We reformulated CounterFact prompts as questions to match the format of our other datasets. Because  
199 we used the TriviaQA probe for the path patching experiment with CounterFact, we also did few-shot  
200 prompting with the prompt from TriviaQA.

### 201 B.1 Licenses

202 Models:

- 203 • Llama 2 is licensed under the Llama 2 Community License Agreement, available at  
204 <https://ai.meta.com/llama/license/>.
- 205 • Llama 3 is licensed under the Meta Llama 3 License, available at  
206 <https://llama.meta.com/llama3/license/>.
- 207 • Gemma 2 is licensed under the Gemma Terms of Use, available at  
208 <https://ai.google.dev/gemma/terms>.

209 Datasets:

- 210 • TriviaQA is licensed under the Apache License 2.0, available at  
211 <https://www.apache.org/licenses/LICENSE-2.0>.
- 212 • WebQuestions is licensed under the Creative Commons Attribution 4.0 International License,  
213 available at <https://creativecommons.org/licenses/by/4.0/>.
- 214 • MMLU (Massive Multitask Language Understanding) is licensed under the MIT License,  
215 available at <https://opensource.org/licenses/MIT>.
- 216 • ARC (AI2 Reasoning Challenge) is licensed under the Creative Commons Attribution-  
217 ShareAlike 4.0 International License, available at <https://creativecommons.org/licenses/by-sa/4.0/>.
- 218 • CounterFact is licensed under the MIT License, available at <https://opensource.org/licenses/MIT>.
- 219

## 220 Appendix C Probe Design

221 We use a  $\mathbb{P}(\text{IK})$  probing approach in part because of the difficulty of reasoning about uncertainty  
222 using token probabilities. Token probabilities for open-ended questions are a highly imperfect proxy  
223 for a model’s confidence, because they conflate semantic uncertainty (uncertainty about content) with  
224 syntactic uncertainty (uncertainty about form). Furthermore, we are most interested in improving  
225 uncertainty quantification for fine-tuned chat models, for which token probabilities do not correspond  
226 to an underlying distribution over possible text strings.

227 We construct a dataset on which to train the  $\mathbb{P}(\text{IK})$  probe according to the following steps.

- 228 1. Perform 32 forward passes for each question on the question-answering task. We used few-shot  
229 prompting with 5 examples to ensure that the model answered in the right format.
- 230 2. Check whether a model’s answers are correct. Specifically, we check whether a model’s answer  
231 contains any correct answer as a substring, ignoring case.
- 232 3. For each question in the dataset, save the number of correct and incorrect answers (implying a  
233 “true probability” of the model answering correctly).
- 234 4. Also, for each question, save the output of the model’s last layer (before the unembedding). This  
235 is a vector in  $\mathbb{R}^{d_{\text{model}}}$ .

236 The  $\mathbb{P}(\text{IK})$  probe is a logistic classifier  $p : \mathbb{R}^{d_{\text{model}}} \rightarrow (0, 1)$  which takes these last layer activations as  
237 input and returns the proportion of correct answers. For example, if the model answers a question  
238 correctly 47% of the time, the probe should output 0.47 when given the last-layer activations at the  
239 last token of that question. We trained with binary cross-entropy loss, using dropout and a triangular  
240 learning rate schedule, and used a low learning rate ( $\eta = 3 \times 10^{-6}$ ) as in [10].

## 241 Appendix D Limitations of Path Patching and Zero-Ablation

242 Path patching and zero-ablation, like many interpretability techniques, yield results which can  
243 imperfectly reflect the contributions of model internals to a task. In particular:

244 **Zero-ablation.** We chose to ablate activations in the model with zeros. While the zero vector is far  
245 from an arbitrary choice, especially given its relevance to dropout and the additive residual structure  
246 of a transformer, this approach may lack specificity. For example, zero-ablating an early or late MLP  
247 layer sometimes severely damages a model’s ability to produce coherent language in general, so  
248 accuracies from ablation do not necessarily correspond to the flow of question-specific information  
249 through the model. Approaches such as causal scrubbing [3] avoid this limitation but are generally  
250 more computationally expensive.

251 **Path patching.** The “path” through the model identified comprises, to a first approximation, the  
252 set of points in the model at which *all* information relevant to the task is present. As such, when  
253 information relevant to a question passes along multiple paths in parallel, it may be that no individual  
254 path shows a substantial difference between the restored and baseline conditions. For example, in the  
255 question in Fig. 2 (left), restoring the input embedding for any one token of “Prince Edward Island”  
256 without the others has little effect on the model.



257 **Appendix E Full Results for Zero-Ablation**

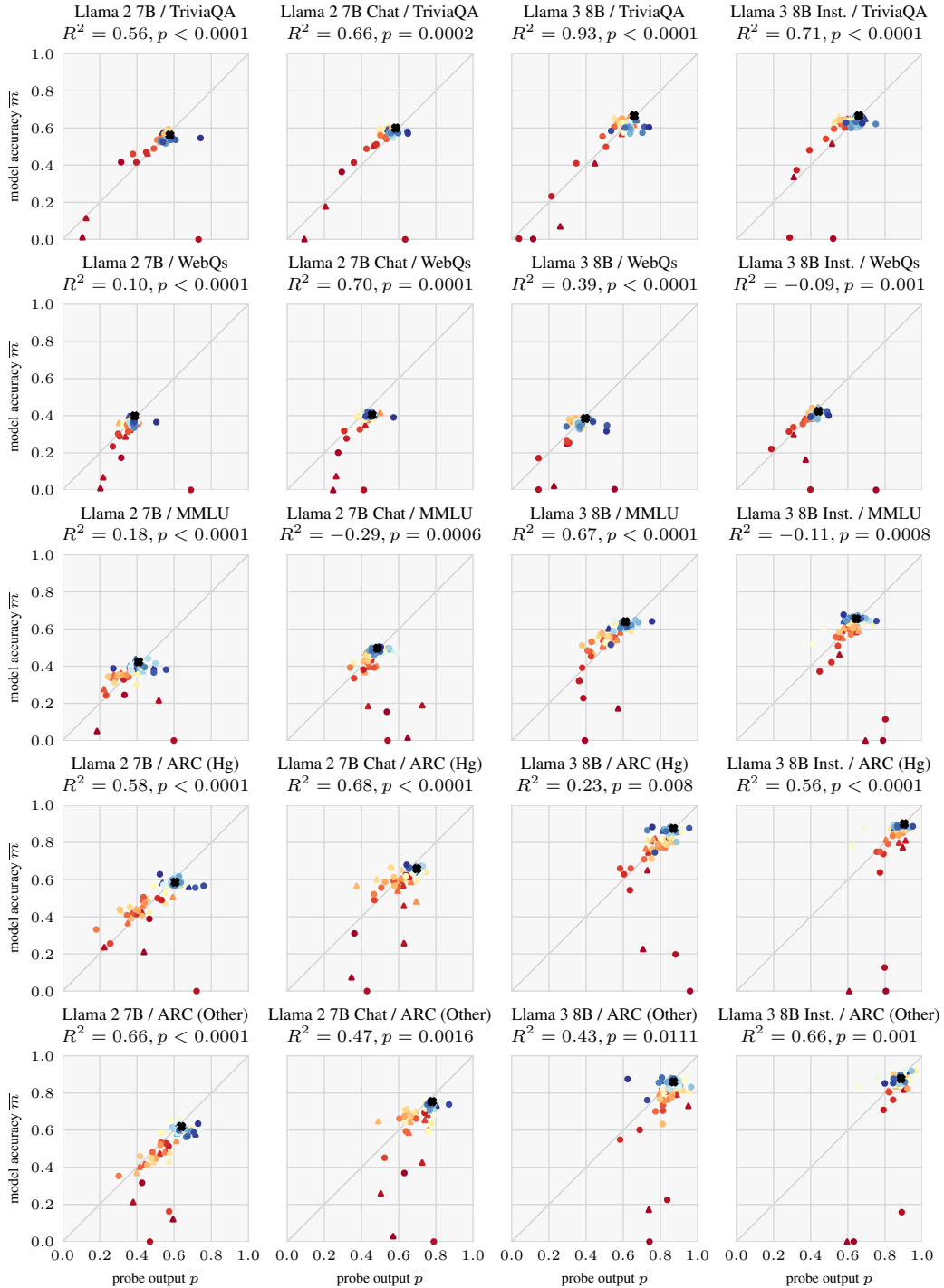


Figure 3: Results of zero-ablation for eight models and five datasets. Circle, triangle, and X markers represent MLP ablations, attention ablations, and clean runs respectively. Warmer colors represent earlier layers. Error bars for individual points are omitted for legibility, but  $\text{std. err.} < 0.032$  in all cases (by the bounds on  $p$  and  $m$ ).

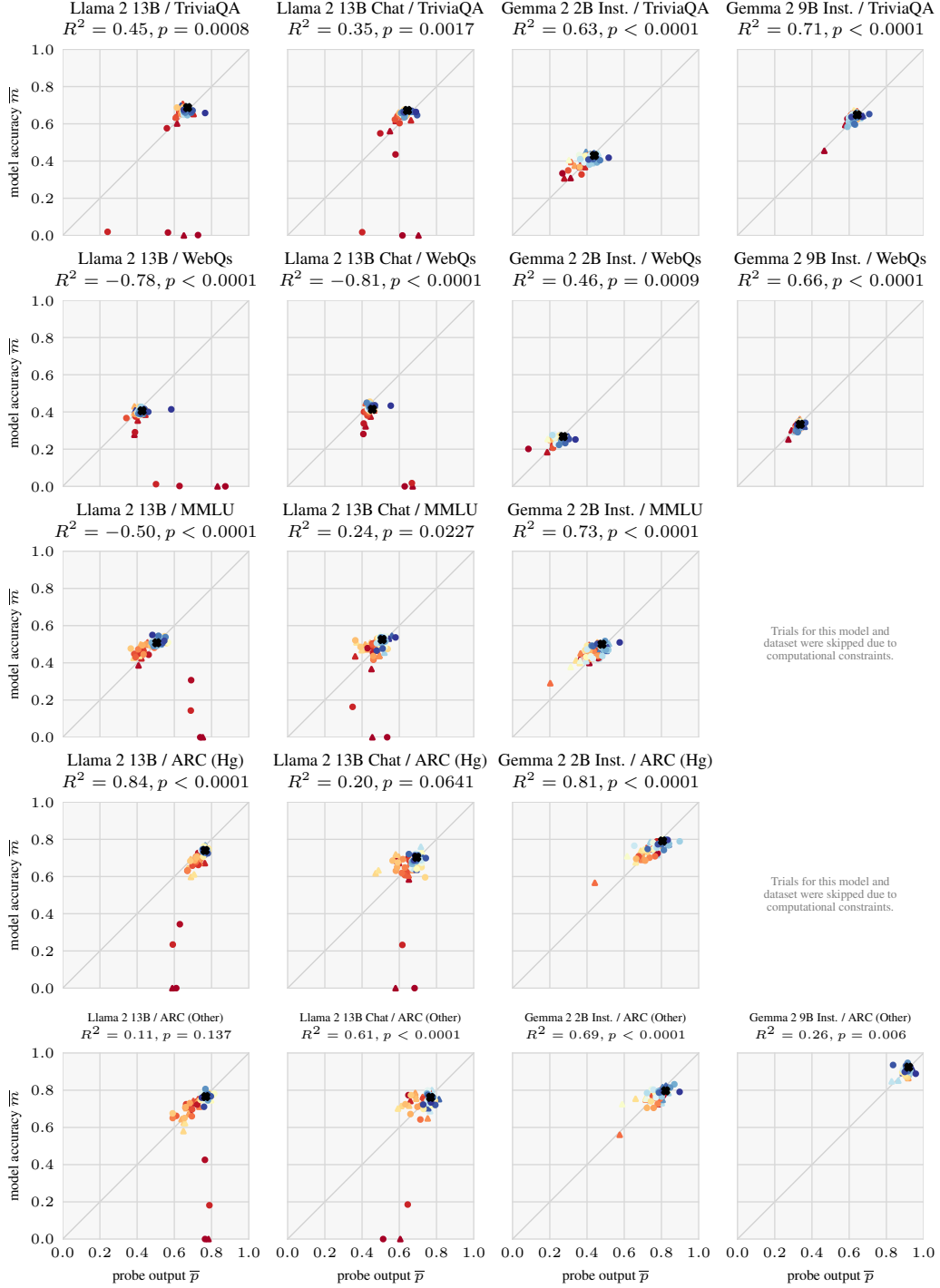


Figure 4: (continued) Results of zero-ablation for eight models and five datasets. Circle, triangle, and X markers represent MLP ablations, attention ablations, and clean runs respectively. Warmer colors represent earlier layers. Error bars for individual points are omitted for legibility, but  $\text{std. err.} < 0.032$  in all cases (by the bounds on  $p$  and  $m$ ).

## 258 **Appendix F Computational Resources**

259 This project has used approximately 1000 GPU-hours of computation time on an academic cluster,  
260 mainly on RTX8000 GPUs with 48 GB of memory, including approximately 500 GPU-hours  
261 for results used directly in this paper. Results for individual model/dataset combinations can be  
262 reproduced independently; for example, the code to produce the TriviaQA / Llama 3 8B Instruct  
263 results ran in approximately 20 GPU-hours.

## 264 **Appendix G Ethics Statement**

265 This paper intends to advance the areas of interpretability and uncertainty quantification for language  
266 models, with the primary aim of making language models more reliable and more trustworthy.  
267 We expect these research directions in general to reduce societal risks from machine learning (for  
268 example, by allowing for warning signals in situations where a model might be lying or making  
269 a dangerous mistake). Nevertheless, since reliability work also makes systems more useful, some  
270 caution is warranted: for example, users might be tempted to deploy the resultant more-reliable  
271 systems in higher-stakes contexts in which tail risks from failures are greater.

272 The humanoid and sciuroid robots in Fig. 1 were created using DALL-E 3.

273 **NeurIPS Paper Checklist**

274 **1. Claims**

275 Question: Do the main claims made in the abstract and introduction accurately reflect the  
276 paper’s contributions and scope?

277 Answer: [Yes]

278 Justification: This paper proposes methods for studying uncertainty quantification in lan-  
279 guage models, and provides evidence for a “shared circuits” hypothesis across a range of  
280 models and tasks; we do not claim to address other settings (e.g., larger models or non-recall-  
281 based questions). Our introduction suggests some potential applications of our methods  
282 (e.g., the study of hallucinations) which we do not claim to pursue these in this paper.

283 **2. Limitations**

284 Question: Does the paper discuss the limitations of the work performed by the authors?

285 Answer: [Yes]

286 Justification: We note the limited range of our experimental settings. We also acknowledge  
287 the major limitations of the mechanistic interpretability techniques we use (in particular,  
288 their tendency to produce noisy results which can be difficult to formalize) in Appendix D,  
289 and note that the hypotheses which we test formally are imperfect proxies for our shared  
290 circuits hypothesis.

291 **3. Theory Assumptions and Proofs**

292 Question: For each theoretical result, does the paper provide the full set of assumptions and  
293 a complete (and correct) proof?

294 Answer: [NA]

295 Justification: We do not present theoretical results.

296 **4. Experimental Result Reproducibility**

297 Question: Does the paper fully disclose all the information needed to reproduce the main ex-  
298 perimental results of the paper to the extent that it affects the main claims and/or conclusions  
299 of the paper (regardless of whether the code and data are provided or not)?

300 Answer: [Yes]

301 Justification: We present novel results based largely on existing mechanistic interpretability  
302 techniques, which we describe in sufficient detail to allow replication. We describe our  
303 probing setup in detail in Appendix C. We also provide code for reproducing our work.

304 **5. Open access to data and code**

305 Question: Does the paper provide open access to the data and code, with sufficient instruc-  
306 tions to faithfully reproduce the main experimental results, as described in supplemental  
307 material?

308 Answer: [Yes]

309 Justification: We provide code for reproducing our work.

310 **6. Experimental Setting/Details**

311 Question: Does the paper specify all the training and test details (e.g., data splits, hyper-  
312 parameters, how they were chosen, type of optimizer, etc.) necessary to understand the  
313 results?

314 Answer: [Yes]

315 Justification: We describe the major details of our experimental setup in the body and  
316 appendices, with full details provided in the code.

317 **7. Experiment Statistical Significance**

318 Question: Does the paper report error bars suitably and correctly defined or other appropriate  
319 information about the statistical significance of the experiments?

320 Answer: [Yes]

321 We describe the statistical tests used for our main results and note the details of our permuta-  
322 tion sampling setup.

### 323 8. Experiments Compute Resources

324 Question: For each experiment, does the paper provide sufficient information on the com-  
325 puter resources (type of compute workers, memory, time of execution) needed to reproduce  
326 the experiments?

327 Answer: [Yes]

328 Justification: Yes, in Appendix F.

### 329 9. Code Of Ethics

330 Question: Does the research conducted in the paper conform, in every respect, with the  
331 NeurIPS Code of Ethics <https://neurips.cc/public/EthicsGuidelines?>

332 Answer: [Yes]

333 Justification: Our work uses commonly-used datasets intended for research and does not  
334 involve human subjects or sensitive data. While this is largely a foundational paper, we  
335 discuss some potential societal impacts and safety implications in Appendix G.

### 336 10. Broader Impacts

337 Question: Does the paper discuss both potential positive societal impacts and negative  
338 societal impacts of the work performed?

339 Answer: [Yes]

340 Justification: While this is largely a foundational paper, we discuss some potential societal  
341 impacts and safety implications in Appendix G.

### 342 11. Safeguards

343 Question: Does the paper describe safeguards that have been put in place for responsible  
344 release of data or models that have a high risk for misuse (e.g., pretrained language models,  
345 image generators, or scraped datasets)?

346 Answer: [NA]

347 Justification: We do not create or release data or models that have a high risk for misuse.

### 348 12. Licenses for existing assets

349 Question: Are the creators or original owners of assets (e.g., code, data, models), used in  
350 the paper, properly credited and are the license and terms of use explicitly mentioned and  
351 properly respected?

352 Answer: [Yes]

353 Justification: Our use of libraries, data, and models is consistent with the relevant licenses  
354 and terms of use. We provide explicit license information in the references section.

### 355 13. New Assets

356 Question: Are new assets introduced in the paper well documented and is the documentation  
357 provided alongside the assets?

358 Answer: [Yes]

359 Justification: We provide documented code for reproducibility.

### 360 14. Crowdsourcing and Research with Human Subjects

361 Question: For crowdsourcing experiments and research with human subjects, does the paper  
362 include the full text of instructions given to participants and screenshots, if applicable, as  
363 well as details about compensation (if any)?

364 Answer: [NA]

365 Justification: This paper does not involve crowdsourcing or human subjects.

### 366 15. Institutional Review Board (IRB) Approvals or Equivalent for Research with Human 367 Subjects

368 Question: Does the paper describe potential risks incurred by study participants, whether  
369 such risks were disclosed to the subjects, and whether Institutional Review Board (IRB)  
370 approvals (or an equivalent approval/review based on the requirements of your country or  
371 institution) were obtained?

372 Answer: [NA]

373 Justification: This paper does not involve crowdsourcing or human subjects.